Monte Carlo simulations of intragrain spin effects in a quasi-2D Heisenberg model with uniaxial anisotropy

2013 J. Phys.: Condens. Matter 25 196004

(http://iopscience.iop.org/0953-8984/25/19/196004)

IOP PUBLISHING JOURNAL OF PHYSICS: CONDENSED MATTER
J. Phys.: Condens. Matter **25** (2013) 196004 (7pp) doi:10.1088/0953-8984/25/19/196004

Monte Carlo simulations of intragrain spin effects in a quasi-2D Heisenberg model with uniaxial anisotropy

M D Leblanc, J P Whitehead and M L Plumer

Department of Physics and Physical Oceanography, Memorial University of Newfoundland, St John's, NF, A1B 3X7, Canada

Received 28 January 2013, in final form 11 March 2013
Published 19 April 2013
Online at stacks.iop.org/JPhysCM/25/196004

Abstract
A combination of Metropolis and modified Wolff cluster algorithms is used to examine the impact of uniaxial single-ion anisotropy on the phase transition to ferromagnetic order of Heisenberg macrospins on a 2D square lattice. This forms the basis of a model for granular perpendicular recording media where macrospins represent the magnetic moment of grains. The focus of this work is on the interplay between anisotropy D, intragrain exchange J' and intergrain exchange J on the ordering temperature T_C and extends our previous reported analysis of the granular Ising model. The role of intragrain degrees of freedom in heat assisted magnetic recording is discussed.

(Some figures may appear in colour only in the online journal)

1. Introduction

The necessity for models of magnetic recording media that go beyond approximations based on the physics at the nanometer length scale is becoming increasingly important not only due to shrinking bit dimensions but also for the evaluation of new paradigms such as heat assisted magnetic recording (HAMR) [1, 2]. The role of degrees of freedom internal to media grains, normally assumed to have uniform magnetization (referred to as the macrospin model), has been shown to be significant in field-induced reversal at temperatures which are comparable to the intrinsic ferromagnetic Curie point [3, 4]. It is at temperatures near T_c that HAMR technology operates. Brute force modeling at the atomic spin scale is straightforward but not practical for large systems [5]. Understanding of the regimes where the uniformly magnetized grain approximation is no longer reliable can be made through studies of how thermal fluctuations affect the interplay between intragrain and intergrain spin ordering and magnetization reversal.

Modern perpendicular recording media is composed of weakly coupled Co-alloy based grains 5–10 nm in dimension, composed of thousands of atomic spins subject to relatively strong uniaxial (hcp) crystalline anisotropy. In our previous study [6], Monte Carlo (MC) simulations were performed on an Ising model of atomic-scale spins for a quasi-2D system of grains, with intragrain ferromagnetic exchange J', coupled by intergrain exchange J. In that work, the macrospin model was referred to as the rigid grain approximation (RGA) and was defined such that all the spins in a grain are perfectly aligned giving a uniform magnetization. This is the fundamental assumption of, for example, micromagnetic simulations. A key measure of the relative importance of intragrain degrees of freedom in this study was the dependence of the system Curie temperature on J and its deviation from the linear dependence expected of the homogeneous 2D Ising model ($J = J'$). The results of kinetic MC simulations of an Ising model of the homogeneous 2D system to represent recording media for HAMR applications have also been reported [7].

In the present work, we improve the previously studied Ising model by replacing it by a Heisenberg system of spins with strong single-ion uniaxial anisotropy D. The dynamics of grain reversal within this more realistic model can be expected to be significantly different than its Ising counterpart [3, 8, 9]. Closely related to this model is the so-called anisotropic exchange model characterized by the difference Δ between exchange involving xy-spins and exchange between the z-components of $\vec{S}_i$. Previous MC simulations have demonstrated that the critical behavior of this model in 2D belongs to the Ising universality class [10].

Related to the present work are several studies of the dependence of T_c on Δ. MC simulations were shown to agree with a modified classical linear spin wave theory yielding a nearly logarithmic dependence on $\Delta < 1$ [11]. Similar results were obtained from later work based on a quantum Green's function approach [12]. A recent high-temperature series expansion study of spin quantum effects in the Heisenberg model with uniaxial anisotropy D on a n-layered square lattice focused on the dependence of T_c on large D values, giving trends similar to the previous works [13]. Somewhat surprisingly, there appears to have been few results on MC simulations of $T_c(D)$ in the classical 2D Heisenberg model with single-ion uniaxial anisotropy, which, as noted by Costa *et al* [14], can be expected to show different phase-transition behavior in 2D from the case of exchange anisotropy.

This paper is organized as follows. In section 2, the homogeneous 2D spin model and quasi-2D model of interacting grains are introduced and a discussion of the combined Metropolis and modified Wolff cluster algorithms are described. Monte Carlo simulation results for the homogeneous 2D model are presented in section 3 for a number of thermodynamic quantities which show anomalies related to the onset of ferromagnetic ordering at different $J = J'$ and D values. Granular model results are presented in section 4 and a scaling relation for T_c versus an effective exchange and effective granular anisotropy is developed and compared with the results of the corresponding macrospin model. Our conclusions are given in section 5.

2. The model

We consider a model consisting of grains on a $L \times L$ square lattice, with each grain represented by a rectangular prism composed of $N_g = L' \times L' \times z$ spins. The total number of spins in the model is thus $N = N_g \times L^2$. Spins within a grain are coupled through near-neighbor intragrain exchange J' (which is set as $J' = 1$) and spins between grains are coupled through intergrain exchange $0 \leq J \leq 1$. Periodic boundary conditions are imposed in the $L \times L$ plane but not in the perpendicular z direction. The homogeneous 2D model is defined by $J = J'$ with $z = 1$, a single layer. Figure 1 shows a schematic model for a system consisting of $L^2 = 9$ grains, each with $(L')^2 = 9$ spins and with $z = 1$. The model Hamiltonian is given by

$$\mathcal{H} = -\sum_{\langle ij \rangle} J_{ij} \vec{S}_i \cdot \vec{S}_j - D \sum_i (S_i^z)^2 \tag{1}$$

with only near-neighbor sites included in the first sum, $\vec{S}_i$ denotes the spin vector at the lattice site i with $|\vec{S}_i| = S$, $J_{ij} = J$ or J', and $D > 0$ is the uniaxial anisotropy strength. Note that the number of nearest-neighbor bonds between each grain is given by $A_g = L' \times z$. High anisotropy media for HAMR applications might have anisotropy values in the range $0.001 < D/J' < 0.01$ [3, 15].

The average magnetization of the Ith grain is given by

$$M_I = \frac{1}{N_g} \left| \sum_{j \in I} \vec{S}_j \right| \tag{2}$$

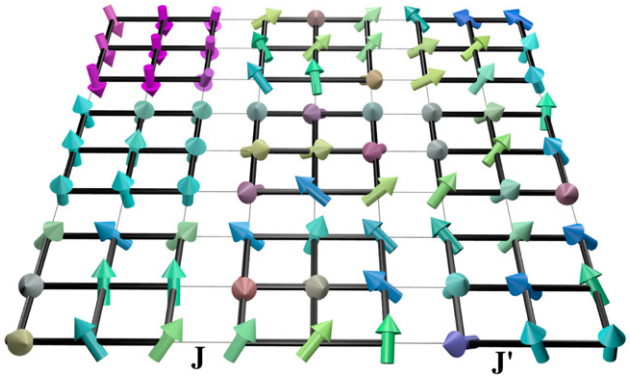

Figure 1. Schematic of the granular Heisenberg model showing $L^2 = 3 \times 3$ grains each composed of $(L')^2 = 3 \times 3$ spins with intragrain exchange J' and intergrain exchange J. Here, $z = 1$ (single layer).

where $\sum_{j \in I}$ is over all N_g spins in grain I. The thermal average magnetization over all grains is thus given for a specific temperature T by

$$M_g(T) = \frac{1}{L^2} \left\langle \sum_I M_I \right\rangle. \tag{3}$$

The total magnetization is defined by

$$M(T) = \frac{1}{N} \left\langle \left| \sum_i \vec{S}_i \right| \right\rangle \tag{4}$$

where i is over all N lattice sites. In addition, the total magnetic susceptibility was calculated using

$$\chi(T) = \beta N (\langle M(T)^2 \rangle - \langle M(T) \rangle^2) \tag{5}$$

where $\beta = 1/T$ and the specific heat is given by

$$C(T) = \frac{\beta^2}{N} (\langle E(T)^2 \rangle - \langle E(T) \rangle^2). \tag{6}$$

For $J \ll 1$ the low-temperature behavior of the model is dominated by the reversal of entire grains. To enhance equilibration, the Metropolis algorithm is combined with a cluster spin algorithm to give good statistics at low temperatures. In this paper we employ a combination of Metropolis and a modified Wolff cluster algorithm [16, 17] in which the probability of extending a cluster from site i to include a neighboring site j is given by $P_{ij} = 1 - e^{-2\beta J_{ij}(\vec{S}_i \cdot \hat{u}_s)(\vec{S}_j \cdot \hat{u}_s)}$, where $\hat{u}_s$ is a seed unit vector used in the algorithm. At low temperatures the clusters formed by the modified Wolff algorithm encompass entire grains, and have an acceptance ratio $\sim e^{-2VD\beta}$, where V denotes the volume of the cluster. In this regime we would expect the granular model to approximate that of the macrospin model. While the inclusion of the anisotropy can lead to a low acceptance ratio for large values of D, the modified Wolff algorithm, when combined with a single spin Metropolis algorithm, was able to provide good statistics for the moderate values of D considered in this paper. In calculating thermodynamic quantities, a single Monte Carlo step (MCS) consisted of

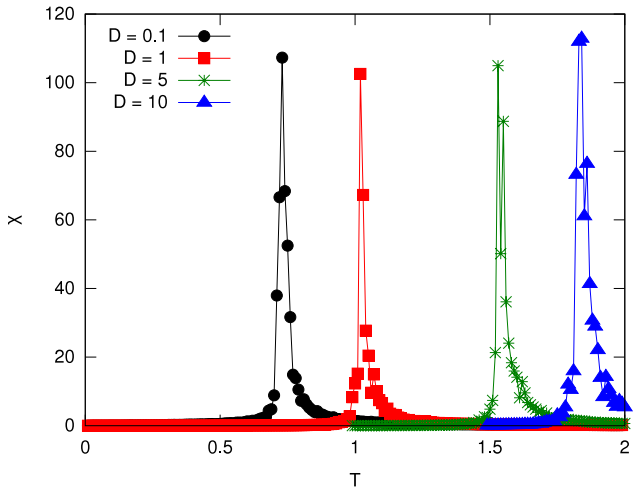

Figure 2. Simulation results for the susceptibility in the homogeneous 2D case at various anisotropy values, using $L = 80$.

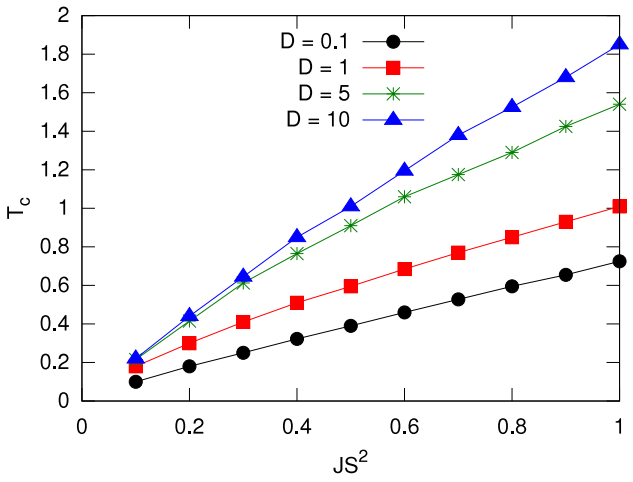

Figure 3. Transition temperature versus exchange for the homogeneous 2D Heisenberg model at various anisotropy strengths.

a Metropolis step attempt for every spin of the lattice followed by a single cluster flip attempt using the modified Wolff algorithm. Typical data were collected averaging around 25 000 MCS, with MCS_0 initial steps discarded for equilibration (typically 10% of MCS). As an initial test of the algorithm, we verified for the 3D Heisenberg model with $D = 0, J = J' = S = 1$, using $L = 10, L' = 1$ and $z = 1$, that the algorithm yields a specific heat anomaly signaling the onset of ferromagnetic order at $T_c/JS^2 = 1.44$, as expected [17].

3. The homogeneous 2D model

We previously examined the behavior of the transition temperature for the case of the Ising model [6]. To assess the effect of the intergranular interaction we compared the transition of the granular model with the corresponding result obtained from a macrospin model with $T_c = 2.269J_{\mathrm{eff}}$, where J_{eff} denotes an effective intergrain exchange interaction given by $J_{\mathrm{eff}} = JA_g = (L'z)J$ (figure 11 of [6]). Extending this analysis to the anisotropic Heisenberg model is complicated by the fact that the transition temperature of the homogeneous 2D anisotropic Heisenberg model is not simply a linear function of the exchange constant, but depends also on the ratio D/J. Moreover, as pointed out in the Introduction, there do not appear to be any analytical or numerical studies that provide reliable estimates for T_c as a function of D. Anisotropy adds new important physics to the present model system, as $D = 0$ has no long range order in 2D or quasi-2D Heisenberg models. As a prelude to our analysis of the results for the granular model we examine the transition temperatures as a function of both exchange and anisotropy for the case of a homogeneous 2D system, $z = 1, L' = 1$ and $J = J'$.

Figure 2 shows representative results for the susceptibility from the homogeneous 2D model with $J = S = 1$, and $L = 80$ at various values of D. From the peaks in these data the critical temperatures can be estimated. Simulations were also performed using a larger range of D values. Figure 3 shows the dependence of T_c on JS^2 at various values of D. Unlike

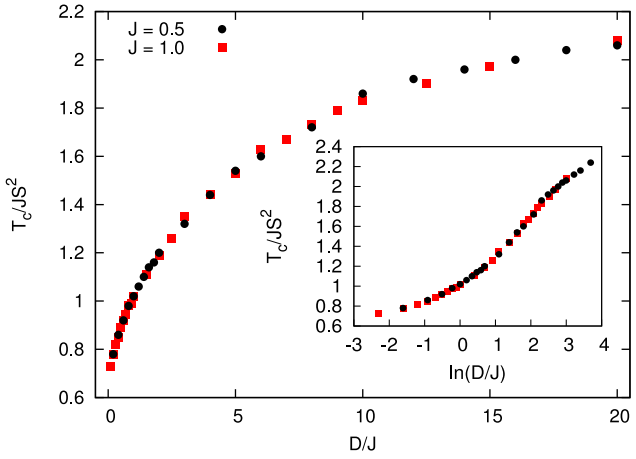

Figure 4. T_c/JS^2 versus D/J, showing the effect of anisotropy strength on the critical temperature for the homogeneous 2D Heisenberg model for two values of $J = J'$ (using $L = 80$ and $L = 160$ for $J = 0.5$ and $J = 1.0$, respectively). Inset shows a semi-logarithmic plot of the same data.

the Ising case, and in contrast with mean-field theory, these $T_c(J)$ plots exhibit clear non-linearity which increases with D. As expected, the overall values of T_c also increase with increasing D.

We also plot in figure 4 the dependence of T_c/JS^2 on D/J for two different values of exchange, $J = 0.5$ and 1.0 and varying anisotropy, $0.001 < D < 20$. As expected, the two data sets collapse onto a single universal curve that is a function of the two variables T_c/JS^2 and D/J. The data show a very strong non-linearity for small values of the ratio D/J. This reflects the effects of the critical fluctuations at the onset of the long range order, which increase as D/J goes to zero, at which point the long range order disappears. Note that in mean-field theory the relation would be $T_c/JS^2 = 1+D/J$. For large D, transverse fluctuations are suppressed and the critical temperature tends to its 2D square-model Ising value, $T_c \approx 2.269JS^2$. Scaling studies of the anisotropic exchange model predict a logarithmic dependence of T_c at small anisotropy

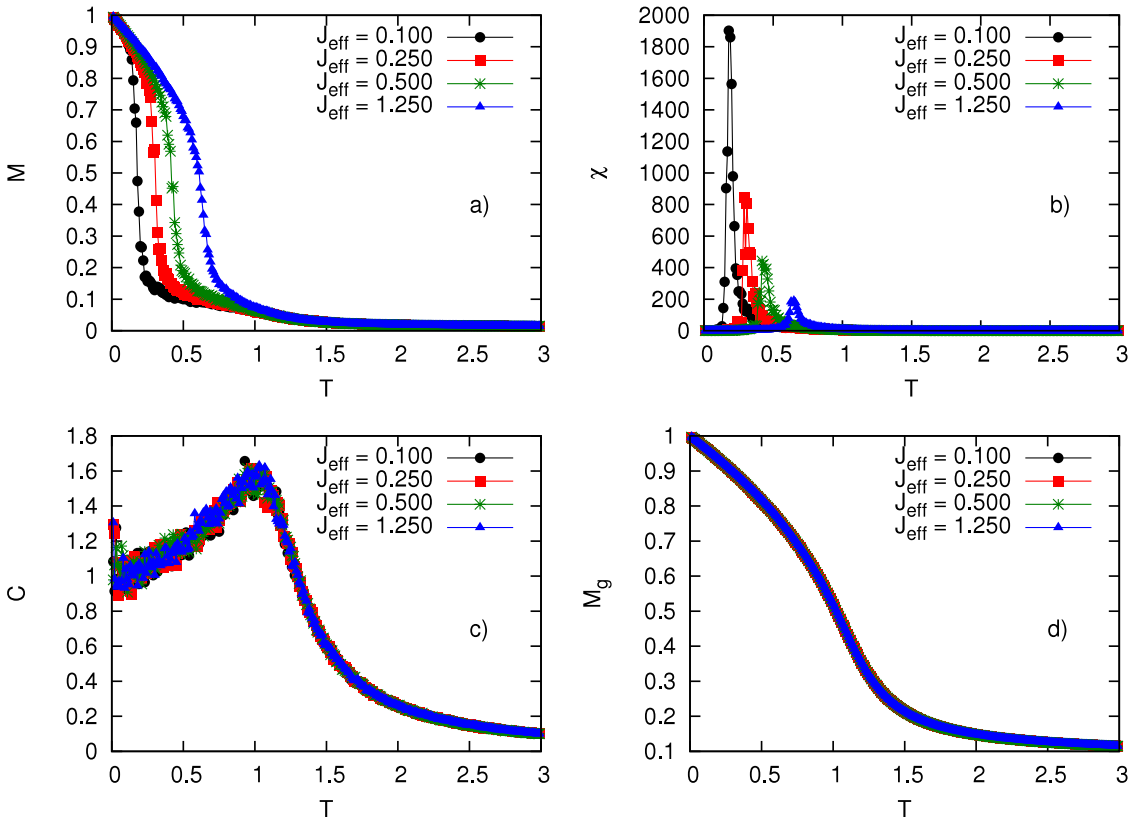

Figure 5. Granular model results for $L = 8$, $L' = z = 5$ and $D = 0.01$, showing total magnetization, susceptibility, specific heat and grain magnetization versus temperature for different values of J_{eff}.

values [18] and for completeness we show our data plotted in this manner in the inset of figure 4. Although a linear behavior at small values of D/J cannot be excluded, this regime is not the focus of the present work and is not necessarily expected in the case of single-ion anisotropy. Numerical studies of these issues have been addressed by other works [10–14].

4. The granular quasi-2D model

In the case of the homogeneous Heisenberg model T_c/JS^2 is no longer constant as it was in the Ising model but is instead a function of D/J as shown in figure 4. Also in the case of the Ising model the fact that the magnitude of the grain magnetization M_g was only weakly temperature dependent for the temperature range of interest allowed us to treat the grain as a macrospin with $S = 1$. In the Heisenberg model the grain magnetization is temperature dependent even down to the lowest temperatures, which will be discussed below (see also figures 5(d) and 6). This can be incorporated into the macrospin model by assigning the macrospin vectors a temperature dependent magnitude $S_{\text{eff}} = M_g(T)$ [19–21]. To determine the range of applicability of the macrospin model in the case of the granular Heisenberg model we therefore study the relationship between $T_c/J_{\text{eff}}M_g^2(T_c)$ and $D_{\text{eff}}/J_{\text{eff}}$ with the data from figure 4 serving as a reference, where D_{eff} is defined as

$$D_{\text{eff}} = (L'^2 z)D. \tag{7}$$

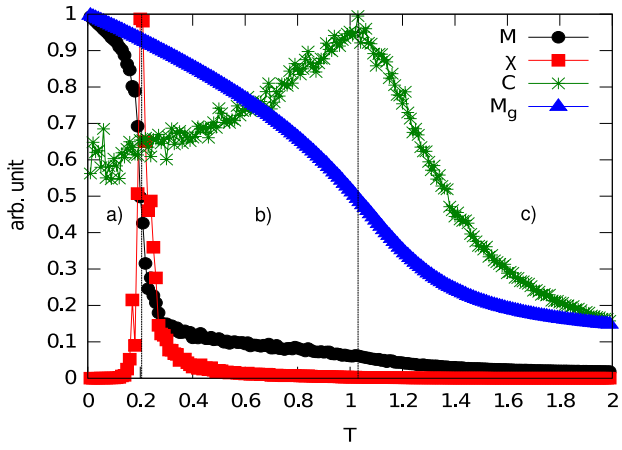

Figure 6. Total magnetization, susceptibility, specific heat and grain magnetization scaled for $L = 8$, $L' = 5$, $z = 5$, $D_{\text{eff}} = 1.25$ and $J_{\text{eff}} = 0.125$. Three regions of different behaviors, region (a): $T < T_c$, region (b): $T_c \leq T \leq T_c'$, and region (c): $T > T_c'$ have spin and macrospin vectors as depicted in figure 7.

Just as in the Ising model, we calculate the temperature dependence of the various thermodynamic values, namely the total magnetization, susceptibility, specific heat and grain magnetization. Figure 5 shows these as a function of temperature for various representative values of intergrain coupling $J = 0.004, 0.01, 0.02$ and 0.05 with $D = 0.01$ and

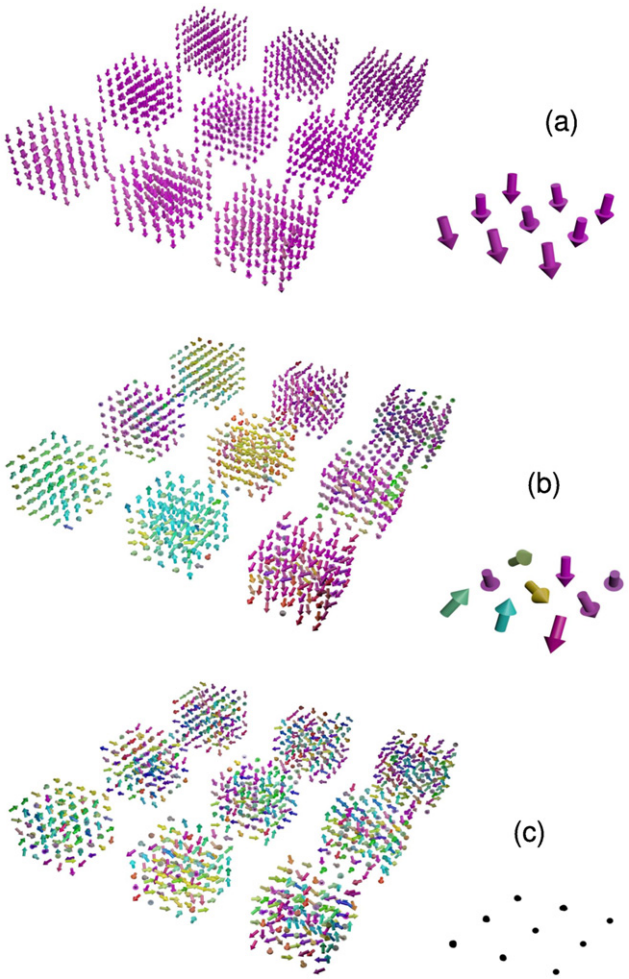

Figure 7. Spin configuration for different temperature regimes, showing several grains of the spin system (left) and the macrospin representation (right) with the same parameters as in figure 6 for: region (a) $T < T_c$, region (b) $T_c \leq T \leq T_c'$, and region (c) $T > T_c'$ (dots represent a grain with almost zero magnetization). The intergrain distance serves only as a visual guide.

$L = 8$ for grains with dimensions $L' = 5$ and $z = 5$, giving $D_{\text{eff}} = 1.25$ and the values of the effective intergrain exchange J_{eff} indicated on the figures.

Figure 5(a) shows the total magnetization curves. Taking the point of inflection in each curve to represent the critical temperature associated with the onset of intergrain ferromagnetic order at $0.25 \lesssim T \lesssim 0.75$, one sees a strong dependence on J. Comparing these results with those from the corresponding Ising model, the enhanced fluctuations of the Heisenberg model are seen to induce a sharper decrease in M at low T for the larger values of J. The magnetic susceptibility, figure 5(b), shows a peak at the critical temperature T_c which corresponds roughly to the point of inflection in the total magnetization curves. As such, these two quantities serve as a means to estimate the value of T_c.

In contrast with the Ising case, the specific heat data of figure 5(c) indicates virtually no dependence on the value of J_{eff}. Rather, there is a peak which occurs at $T \approx 1.05$, which we label T_c', corresponding to the intragrain ordering temperature. Note that, except for enhanced noise at very low T due to lower acceptance rates as the Boltzmann factor becomes very small, the specific heat tends to unity for $T \to 0$, as expected of Heisenberg models. The intragrain order is also clear from figure 5(d) showing that the grain magnetization has a point of inflection at the same T_c', also independent of J_{eff}. Notably, unlike the Ising case, $M_g(T)$ also exhibits a large slope even at very low T.

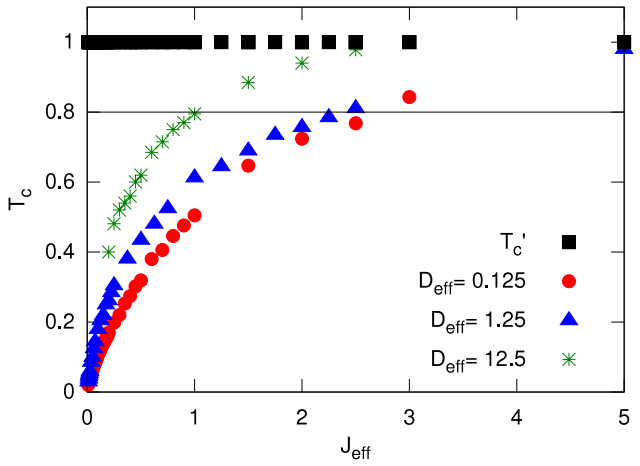

Figure 8. Critical temperature versus effective exchange comparing the granular Heisenberg model with different anisotropy strengths to the homogeneous 2D model with $L' = 5$, $z = 5$, and $L = 8$. the horizontal line at 0.8 estimates the region above which the macrospin model would break down.

The total magnetization and specific heat allow for a good estimation of intergrain order T_c whereas the grain magnetization and specific heat can be used to obtain the intragrain ordering temperature T_c'. Shown in figure 6 are results for one value of $J = 0.005$ with all of these (normalized) quantities on the same graph. There are three different regions of interest, corresponding to (a): $T < T_c$, (b) $T_c \leq T \leq T_c'$, and (c) $T > T_c'$.

At high temperatures in region (c), the system is paramagnetic and all the spins are randomly oriented. As the temperature decreases below T_c' in region (b), the spins inside grains start ordering and individual grains can often be considered to have most spins pointing in one direction. When the temperature decreases even more to below T_c (region (a)), the total and grain magnetization are both near unity, as the grains order amongst themselves. This is seen in figure 7, where the spin configuration of the system in these different regions is shown along with their grain-level macrospin representation.

To obtain more meaningful results, additional simulations were run on a system with the same dimensions as above using the anisotropy values $D_{\text{eff}} = 0.125$, 1.25 and 12.5, with varying J_{eff}. Figure 8 shows how T_c and T_c' vary as a function of J_{eff}. The data show $T_c' \sim 1$ is almost independent of J_{eff} while T_c increases rapidly until T_c and T_c' merge, beyond which the intra- and intergrain ordering occur simultaneously, with T_c increasing more slowly with increasing J_{eff}. The data also show that, for J_{eff} fixed, T_c increases with increasing D_{eff}, rising rapidly until T_c and T_c' coincide at which point it flattens off.

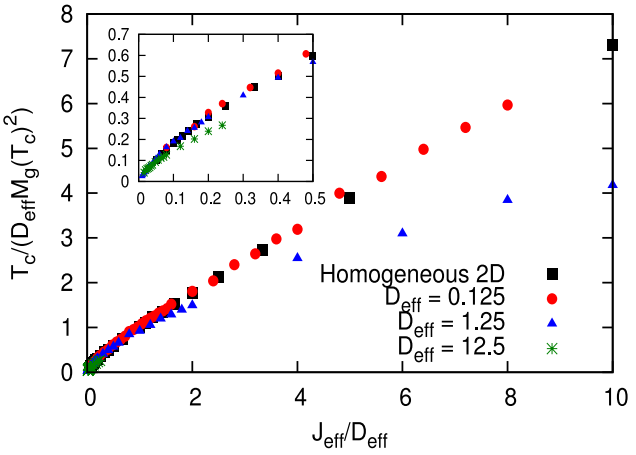

Figure 9. Reduced and normalized critical temperature versus reduced anisotropy comparing the granular Heisenberg model to the homogeneous 2D model with $L' = 5$, $z = 5$, $L = 8$, for a range of values of $D_{\rm eff}$.

The same data is also presented in figure 9 with $T_{\rm c}/D_{\rm eff}M_{\rm g}^2(T_{\rm c})$ plotted as a function of $J_{\rm eff}/D_{\rm eff}$ together with the results presented in figure 4 for the homogeneous 2D Heisenberg model. For the low anisotropy case, $D_{\rm eff} = 0.125$, the data for the granular Heisenberg model track the results of the homogeneous model over the entire range of $J_{\rm eff}/D_{\rm eff}$ shown in the graph and beyond to $J_{\rm eff}/D_{\rm eff} = 20$. This implies that for $D_{\rm eff} = 0.125$ the macrospin model in which the macrospin describing the grains have a magnitude $S_{\rm eff} = M_{\rm g}(T)$, an effective anisotropy constant $D_{\rm eff} = (L'^2 z)D$ and an effective nearest-neighbor coupling constant $J_{\rm eff} = L'zJ$ are consistent with the granular Heisenberg model for the range of temperatures and parameters considered in the present work.

For $D_{\rm eff} = 1.25$, the results from the granular Heisenberg model presented in figure 9 track the homogeneous model only up to $J_{\rm eff}/D_{\rm eff} \sim 2$, corresponding to a value of $J_{\rm eff} \sim 2.5$. From figure 8 we see that this corresponds to a ratio of $T_{\rm c}/T_{\rm c}' \sim 0.8$, thus we see in analogy with the earlier work on the Ising model that the macrospin model breaks down as $T_{\rm c}$ approaches $T_{\rm c}'$ due to the intragrain fluctuations. If we assume this ratio $T_{\rm c}/T_{\rm c}' \sim 0.8$ defines in some qualitative sense the limit for the applicability of the macrospin model then we obtain from figure 8, for $D_{\rm eff} = 0.125$, a value of $J_{\rm eff} \sim 2.5$. This would therefore imply that for $D_{\rm eff} = 0.125$ the macrospin model would be applicable up to $J_{\rm eff}/D_{\rm eff} = 2.5/0.125 = 20$, a result consistent with the comparison of the granular Heisenberg model and the macrospin model discussed above.

Applying the same criteria to the high anisotropy case $D_{\rm eff} = 12.5$, we obtain from figure 8 that $T_{\rm c}/T_{\rm c}' = 0.8$ corresponds to a value of $J_{\rm eff} \sim 1$. This would imply that the macrospin model would break down for $J_{\rm eff}/D_{\rm eff} \sim 1/12.5 \sim 0.08$. While high anisotropy data shown in the inset of figure 9 are fairly noisy they nevertheless show $T_{\rm c}/D_{\rm eff}M_{\rm g}^2(T_{\rm c})$ tracking the homogeneous Ising model fairly well up to that point.

While the deviation of the curves plotting $T_{\rm c}/D_{\rm eff}M_{\rm g}^2(T_{\rm c})$ against $J_{\rm eff}/D_{\rm eff}$ for the granular Heisenberg model from the corresponding macrospin results given in figure 4 is less marked than the results seen in the Ising model [6], they are nevertheless adequate to estimate the range of the applicability of the macrospin approximation in the present case. The above analysis would therefore suggest that, provided the macrospin model is modified to include the temperature dependence of the grain magnetization $M_{\rm g}$, it appears to provide a reasonable account of the static properties of the granular Heisenberg model when $T_{\rm c} \lesssim 0.8\ T_{\rm c}'$ for at least the temperatures and parameters considered.

5. Conclusions

In this paper, Monte Carlo simulation results are presented to illustrate the effect of intragrain spin fluctuations for the ferromagnetic Heisenberg model with single-ion uniaxial anisotropy on a stacked square lattice. The simulations combine a modified Wolff cluster algorithm with the single spin Metropolis algorithm. This work represents an extension of our previous study of a corresponding Ising model [6], where a deviation between transition temperatures of macrospin and granular models occurs as intergrain exchange coupling J increases. It includes the dependence of the ratio of $T_{\rm c}/JS^2$ on J/D and the effect of the enhanced fluctuations on the temperature dependence of the grain magnetization $M_{\rm g}(T)$, that are relevant to the study of the Heisenberg model. In analogy to the earlier work on the Ising model the method provides an estimate of the limit of the applicability of the macrospin model. In the case of the Heisenberg model this is given by the requirement that coupling between the grains should be such that $J_{\rm eff}$ is selected so that $T_{\rm c} \lesssim 0.8\ T_{\rm c}'$. This is in contrast with our corresponding estimate for the Ising model $T_{\rm c} \lesssim 0.5\ T_{\rm c}'$ [6].

A goal in the design and fabrication of modern recording media is to reduce intergrain exchange, as this leads to a reduction in so-called transition noise [22]. Typically, intergrain exchange is a factor of about 100–1000 smaller than intragrain exchange so that HAMR targeted media might correspond to a ratio of anisotropy to exchange in the range $0.1 < D_{\rm eff}/J_{\rm eff} < 10$. For modeling efforts at zero temperature, the macrospin (RGA) approximation can thus be expected to be valid. However, the present work suggests that even for room temperature modeling of materials such as Fe–Pt with $T_{\rm c}' \simeq 800$ K, [15] the macrospin approximation is questionable and is certainly not appropriate when the material is heated close to $T_{\rm c}'$, as in the HAMR process, even with the temperature dependence of the magnetic moment of the grains included. To properly account for the impact of internal spin degrees of freedom on switching behavior of grain magnetization vectors under the influence of an applied magnetic field and thermal fluctuations requires the application of the more sophisticated atomistic calculations [3] or the Landau–Lifshitz–Bloch formalism [23]. Such methods include a more complete account of the internal spin degrees of freedom on both the static and dynamic properties of these high anisotropy materials.

Acknowledgments

This work was supported by the Natural Sciences and Engineering Research Council (NSERC) of Canada, the Canada Foundation for Innovation (CFI), and the Atlantic Computational Excellence network (ACEnet).

References

[1] Rottmayer R E *et al* 2006 *IEEE Trans. Magn.* **42** 2417
[2] Plumer M L, van Ek J and Cain W C 2011 *Phys. Can.* **67** 25
[3] Mercer J I, Plumer M L, Whitehead J P and van Ek J 2011 *Appl. Phys. Lett.* **98** 192508
[4] Evans R F L, Hinzke D, Atxitia U, Nowak U, Chantrell R W and Chubykalo-Fesenko O 2012 *Phys. Rev.* B **85** 014433
[5] Thompson S H, Brown G, Kuhnle A D, Rikvold P A and Novotny M A 2009 *Phys. Rev.* B **79** 024429
[6] Leblanc M D, Plumer M L, Whitehead J P and Mercer J I 2010 *Phys. Rev.* B **82** 174435
[7] Deskins W R, Brown G, Thompson S H and Rikvold P A 2011 *Phys. Rev.* B **84** 094431
[8] Rohart S, Campiglio P, Repain V, Nahas Y, Chacon C, Girard Y, Lagoute J, Thiaville A and Rousset S 2010 *Phys. Rev. Lett.* **104** 137202
[9] Ouazi S, Wedekind S, Rodary G, Oka H, Sander D and Kirschner J 2012 *Phys. Rev. Lett.* **108** 107206
[10] Binder K and Landau D P 1976 *Phys. Rev.* B **13** 1140
[11] Serena P A, García N and Levanyuk A 1993 *Phys. Rev.* B **47** 5027
Gouvêa M E, Wysin G M, Leonel S A, Pires A S T, Kamppeter T and Mertens F G 1999 *Phys. Rev.* B **59** 6229
[12] Hu A-Y and Chen Y 2008 *Physica* A **387** 3471
[13] Pan K-K 2012 *Physica* A **391** 1984
[14] Costa B V and Pires A S T 2003 *J. Magn. Magn Mater.* **262** 316
[15] Kryder M 2008 *IEEE Trans. Magn.* **96** 1810
[16] Newman M E J and Barkema G T 1999 *Monte Carlo Methods in Statistical Physics* (Oxford: Oxford University Press)
[17] Chen K, Ferrenberg A M and Landau D P 1993 *Phys. Rev.* B **48** 3249
[18] Nelson D R and Pelcovits R A 1977 *Phys. Rev.* B **16** 2191
Pelissetto A and Vicari E 2007 *Phys. Rev.* B **76** 024436
[19] Li Z, Wei D and Wei F 2008 *J. Magn. Magn. Mater.* **320** 3108
[20] Torabi A, van Ek J, Champion E and Wang J 2009 *IEEE Trans. Magn.* **45** 3848
[21] Plumer M L, van Lierop J, Southern B W and Whitehead J P 2010 *J. Phys.: Condens. Matter* **22** 296007
[22] Plumer M, van Ek J and Weller D (ed) 2001 *The Physics of Ultra-High-Density Magnetic Recording* (Berlin: Springer)
[23] Bunce C, Wu J, Ju G, Lu B, Hinzke D, Kazantseva N, Nowak U and Chantrell R W 2010 *Phys. Rev.* B **81** 174428
Kilic U, Finocchio G, Hauet T, Florez S H, Aktas G and Ozatay O 2012 *Appl. Phys. Lett.* **101** 252407